Available online at www.sciencedirect.com

ScienceDirect

Ceramics International 40 (2014) 263–271

CERAMICS INTERNATIONAL

www.elsevier.com/locate/ceramint

Application of the statistical Taguchi method to optimize X-SiAlON and mullite formation in composite powders prepared by the SRN process

Amin Jamshidi[a], Amir Abbas Nourbakhsh[b,*], Sanaz Naghibi[b], Kenneth J.D. MacKenzie[c]

[a]Department of Materials Engineering, Najafabad Branch, Islamic Azad University, Isfahan, P.O. Box: 517, Iran
[b]Department of Ceramic Engineering, Shahreza Branch, Islamic Azad University, Isfahan, P.O. Box: 311-86145, Iran
[c]MacDiarmid Institute for Advanced Materials and Nanotechnology, School of Chemical and Physical Sciences, Victoria University of Wellington, Wellington, New Zealand

Received 15 February 2013; received in revised form 1 May 2013; accepted 20 May 2013
Available online 7 June 2013

Abstract

The formation of an X-sialon/mullite nanocomposite by a combination of mechanical activation and silicothermal reduction and nitridation is reported. The starting materials (andalusite, Si and various aluminium sources) were activated in a planetary mill and fired in N_2 at 1450 °C. Microstructure and phase analysis was carried out on fired and unfired samples using X-ray diffraction (XRD), scanning electron microscopy (SEM) and energy dispersive X-ray spectroscopy (EDS). Taguchi statistical experiments were carried out to optimize the formation and crystallinity of the X-sialon component of the sialon–mullite composite. The milling time is the factor of greatest influence on the formation and crystallite size of X-sialon; milling for 15 h increases the amount of X-sialon formed but longer milling times decrease the crystallinity of the products and the sialon/mullite ratio. High-energy milling of an andalusite/Si/alumina mixture produces a mullite-sialon nanocomposite powder. TiO_2 additive stabilises the mullite component whereas Y_2O_3 enhances the formation of X-sialon and $Al(OH)_3$ increases the crystallinity. The optimized conditions for the production of X-sialon/mullite nanocomposite powders are the use of Al_2O_3 as the Al source, milling time 15 h, avoiding the use of TiO_2 as an additive.

Keywords: D. Mullite; X-Sialon; Silicothermal reduction and nitridation; Taguchi analysis

1. Introduction

Ceramic matrix nanocomposites have attracted a great deal of attention from researchers due to their numerous technological applications. There are two general categories of nanocomposites, one type containing only nanometer sized grains and the other consisting of nanosized particles distributed with micron-sized grains [1]. Various techniques have been used to prepare nanocomposite powders, including mechanical mixing of powders, mechanosynthesis, vapour deposition, chemical vapour condensation, hydrothermal precipitation, sol–gel methods and spray pyrolysis [2].

Oxide-nonoxide ceramic composites are of considerable interest nowadays. Previously reported nanocomposites include Si_3N_4–mullite–Al_2O_3 nanocomposites synthesized by a reaction sintering method [1], mullite-SiC nanocomposites fabricated by a sol–gel route [3] and a mullite–sialon–alumina composite prepared by an infiltration process [4].

Sialons are phases in the Si–Al–O–N system and have excellent properties such as high hardness and mechanical strengths at low and high temperatures, low thermal expansion coefficients, good resistance to wear, and chemical resistance in a number of corrosive environments. One of their least favourable properties is their resistance to oxidation. X-sialon is a sialon phase with a high oxygen content; its synthesis by a

*Corresponding author. Tel.: +98 321 3232706; fax: +98 321 3232702.
E-mail addresses: amin_jam_g@yahoo.com (A. Jamshidi), nourbakhsh@iaush.ac.ir (A.A. Nourbakhsh), naghibi@iaush.ac.ir (S. Naghibi), kenneth.MacKenzie@vuw.ac.nz (K.J.D. MacKenzie).

0272-8842/$ - see front matter © 2013 Elsevier Ltd and Techna Group S.r.l. All rights reserved.
http://dx.doi.org/10.1016/j.ceramint.2013.05.133

reduction reaction does not therefore require a strong reducing agent such as carbon. The most popular route to synthesize X-sialon is by silicothermal reduction and nitridation (SRN) of aluminosilicates [5–8]. SRN is a one-step method to produce an X-sialon body [6]. SRN of an aluminosilicate which follows four separate steps; decomposition of the aluminosilicate to form mullite and amorphous silica, nitridation of the elemental Si, reaction between the aluminium source and the amorphous silica and finally the formation of a solid solution of Si_3N_4 and mullite to form X-sialon. In the first step, the formation of a gas-impermeable product layer around the partially reacted Si grains causes the nitridation reaction to become markedly slower and occur in two steps. In the presence of Y_2O_3, the nitridation reactions proceed faster and in one-step. In the final step, the presence of Y_2O_3 causes the mullite to be removed at lower temperatures with the formation of X-sialon. Thus, the action of Y_2O_3 is to increase the reaction rate without significantly changing the reaction sequence [5]. The effect of 1 wt% of other additives such as MgO, CaO, BaO, Fe_2O_3, Y_2O_3, ZrO_2 and CeO_2 on the SRN process has been investigated. It is reported that the first step (nitridation of the Si) is facilitated by all above oxides but especially by Fe_2O_3 and BaO. The second step (mullite formation) is promoted by Y_2O_3 and ZrO_2 but delayed by CaO and MgO. The fourth step (X-sialon formation) is most marked in the presence of Y_2O_3, CaO and MgO, but is suppressed by Fe_2O_3, which enters and stabilises the mullite structure. The beneficial effects of Y_2O_3 and MgO are related to their formation of liquid phases at the reaction temperature. The most favourable additives for promoting both X-sialon formation and densification are Y_2O_3, CaO and CeO_2 followed by MgO [6]. The trends in the formation of mullite and subsequent X-sialon are essentially independent of the additive concentration (1 and 10 wt% MgO, Y_2O_3 and Fe_2O_3) whereas the density is increased by an increase in the additive content [7]. In other research, MacKenzie et al. compared γ-Al_2O_3 with $Al(OH)_3$ as the Al source in the SRN process under mechanochemical activation, showing that substitution of γ-Al_2O_3 by $Al(OH)_3$ facilitates the production of Al–O–Si bonds during grinding and increases the degree of crystallinity, whereas ground samples containing γ-Al_2O_3 showed a greater tendency to convert to X phase sialon [9].

Mullite is an attractive oxide ceramic because of its high melting point (1850 °C), good mechanical properties, low thermal conductivity, low thermal expansion and good chemical stability. The influence of additives on the formation of mullite from aluminosilicates has previously been reported [10–13]. Since mullite formation is an inevitable step in the SRN process [5] and the crystal structures of mullite and X-sialon are similar [14], the relative amounts and morphology of these phases in powders synthesized by the SRN process could be an important factor in determining the ultimate properties of composite powders. X-sialon formation is also governed by the starting materials, preparation technique and firing temperature, and the additional formation of other phases such as Si_3N_4, mullite, and O-sialon have been reported [5–7].

The present research investigated the formation of X-sialon containing nanocomposite powders. To achieve nanosized particles, the raw materials were ground in a planetary mill, then subjected to silicothermal reduction and nitridation to obtain X-sialon. The ease of synthesis of the resulting X-sialon containing composites and the influence of different synthesis variables was optimized by a series of experiments based on Taguchi methodology.

2. Material and methods

The starting materials were 50–350 μm andalusite (Kerphalite KF, Damrec, Paris, France), 63–200 μm α-alumina, < 150 μm aluminium hydroxide and ~40 μm Al powder (Merck, Frankfurt, Germany), < 10 μm Si powder (Sicomill, Kema Nord Engineering Ceramics, Ljungaverk, Sweden), ~10 μm Y_2O_3 (Alfa Aesar, Johnson Matthey, Reacton®, London, England) and 21 nm TiO_2 (Degussa® P_{25}, Evonik, Essen, Germany).

The influence of different factors on the phase composition and crystallinity of the composite samples were assessed by designing an orthogonal experimental based on the Taguchi method with three factors each of the three levels as shown in Table 1. Powder blends were prepared from appropriate mixtures to provide the samples described in Table 2. The powder mixtures were milled in a planetary mill at 600 rpm with alumina balls ($Ø = \sim 2$ mm) in a Teflon container with a balls-to-powder weight ratio of 20. To prevent oxidation the milling pot was filled with high-purity nitrogen gas and the mill was stopped and allowed to cool for 15 min after each 1 h of grinding. In samples 3, 6 and 9, in which the aluminium source was metallic Al powder, the mixture was cooled slowly under nitrogen after milling to prevent aluminothermic reactions. Upon reaching room temperature the Al reacted with O_2 to form Al_2O_3 without oxidation of Si (this was demonstrated by XRD).

The milled mixtures were fired in a horizontal laboratory tube furnace under flowing nitrogen (50 mL/min) at a heating rate of 10 °C/min to 1100 °C, and then at 2 °C/min to 1450 °C. The furnace was cooled immediately on reaching the maximum temperature.

The morphology and elemental compositions of the powders were determined by SEM/EDS (XL30, Philips, Amsterdam, Netherlands, operating at 17 kV in the secondary electron imaging mode). The powder samples were coated with Au using a BAL-TEC SCD005 sputter coater prior to imaging.

Transmission electron microscopy and selected area electron diffraction (TEM-SAED, Philips) was carried out at 100 kV.

XRD analysis of the samples was carried out using a D8 Advance spectrometer (Bruker, Karlsruhe, Germany) with Cu radiation ($K\alpha = 1.540598$) and a Ni filter. The diffraction traces

Table 1
Factors and levels for the experimental design.

Factors	Additive	Al Source	Milling time (h)
Levels	–	$Al(OH)_3$	0
	Y_2O_3	α-Al_2O_3	30
	TiO_2	Al	15

Table 2
Series of experiments required.

Sample code	Factors			Sample component
	Additive (5 wt%)	Al Source	Milling time (h)	
1	–	$Al(OH)_3$	0	$Al_2O_3.SiO_2$+Si+$Al(OH)_3$
2	–	α-Al_2O_3	30	2($SiO_2.Al_2O_3$)+2Si+Al_2O_3
3	–	Al	15	$Al_2O_3.SiO_2$+Si+Al
4	Y_2O_3	$Al(OH)_3$	30	$Al_2O_3.SiO_2$+Si+$Al(OH)_3$
5	Y_2O_3	α-Al_2O_3	15	2($SiO_2.Al_2O_3$)+2Si+Al_2O_3
6	Y_2O_3	Al	0	$Al_2O_3.SiO_2$+Si+Al
7	TiO_2	$Al(OH)_3$	15	$Al_2O_3.SiO_2$+Si+$Al(OH)_3$
8	TiO_2	α-Al_2O_3	0	2($SiO_2.Al_2O_3$)+2Si+Al_2O_3
9	TiO_2	Al	30	$Al_2O_3.SiO_2$+Si+Al

were analyzed using PANalytical X'Pert HighScore software in conjunction with the JCPDS database.

The numerical data required for the statistical analyses were derived from XRD estimations of the amounts of the phases present and their crystallinity. Although this did not provide absolute numerical values, the comparative data illustrate the influence of the various parameters and are therefore suitable for the present purpose. Crystalline materials result in sharp XRD patterns whereas amorphous phases, lattice strain and small particle sizes lead to broadening of the XRD peaks. The degree of crystallinity can be accessed from the ratio of the peak area arising from the crystalline part of sample to the total pattern area [15]. The peak area and total pattern area were obtained from the X'Pert software, and can be compared from sample to sample, provided the patterns are obtained under similar instrumental conditions. To calibrate this method, the backgrounds of the peaks were calculated by setting the crystallinity of the Al, Si, TiO_2 and andalusite starting materials at $100 \pm 1\%$. The approximate degree of crystallinity was determined in this way. The mass fractions of the identified phases were calculated by the matrix flushing model [16] using values of the scale factor (SF) and reference intensity ratio (RIR) values from the X'Pert software database.

As mentioned above, greater amounts of X-sialon of a higher degree of crystallinity were desirable. On the other hand, mullite formation is an inevitable step in the SRN process [5] and the presence of some residual mullite could have a positive effect on the synthesized composite. For this reason, an index named *Response* was defined in Eq. (1);

$$Response = \frac{Degree\ \ of\ \ Crystallinity \times \%X\text{−Sialon}}{\%\ \ Mullite} \quad (1)$$

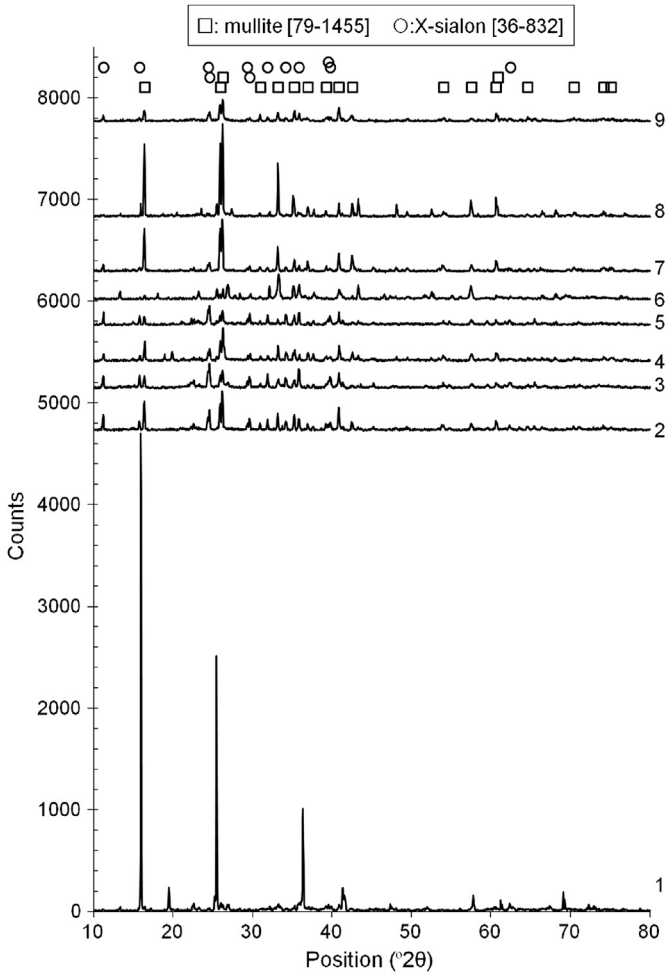

Fig. 1. XRD patterns of powder samples. The squares refer to mullite [79-1455] and the circles show the main peaks of X-sialon [36-832].

3. Results and discussion

3.1. Phase composition and morphology

The XRD patterns of all the samples are shown in Fig. 1. All the samples contain a mixture of mullite and X-sialon, apart from samples 1, 6 and 8 which also contain small amounts of β-sialon. Other phases such as Al_2O_3, Si_3N_4 and $Y_2(Si_3O_3N_4)$ are formed during firing. Semiquantitative estimates of the relative phase contents and the degree of crystallinity are shown in Fig. 2. According to the numerical data in Fig. 2 and based on the Taguchi method using an L_9 orthogonal array, the influence of the sample design parameters on the degree of crystallinity, percentage of X-sialon, percentage of mullite and response are shown in Fig. 3 and Table 3.

Sample 1 (containing no additive and unmilled) retains a high percentage of andalusite after firing under N_2 atmosphere,

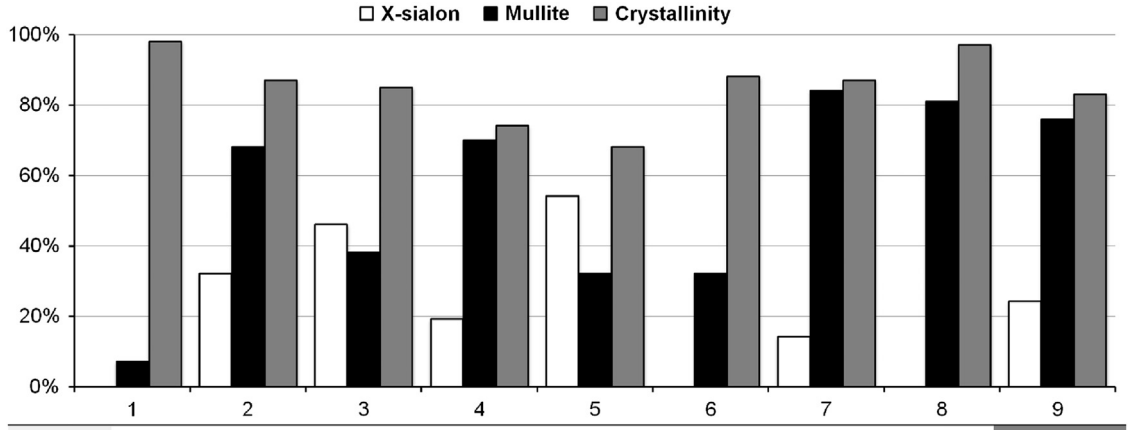

Sample	X-sialon	Mullite	Andalusite	β-sialon	Si_3N_4	Al_2O_3	$Y_2(Si_3O_3N_4)$	$Y_3Al_5O_{12}$	TiO_2	Crystallinity
1	0	7	90	3	0	0	0	0	0	98
2	32	68	0	0	0	0	0	0	0	87
3	46	38	0	0	16	0	0	0	0	85
4	19	70	0	0	0	9	2	0	0	74
5	54	32	0	0	0	8	6	0	0	68
6	0	32	0	28	0	28	0	12	0	88
7	14	84	0	0	0	0	0	0	2	87
8	0	81	0	0	0	17	0	0	2	97
9	24	76	0	0	0	0	0	0	0	83

Fig. 2. The amounts of mullite, X-sialon and crystallinity of the 9 samples.

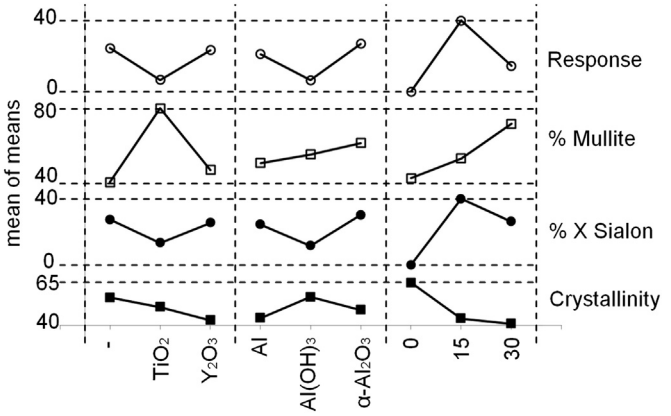

Fig. 3. Influence of design parameters on the degree of crystallinity, percentage of X-sialon, percentage of mullite and response.

but the degree of crystallinity in this sample was the highest of all the samples (Fig. 2). It appears that the lack of additives and milling, and the relatively low firing temperature is responsible for the stability of the andalusite, which does not survive in the other samples containing additives such as Y_2O_3 and TiO_2 and/or milled. The XRD pattern of sample 1 did not exactly match andalusite or mullite; comparison of the pattern of sample 1 and the andalusite starting material (Fig. 4) show that sample 1contains predominantly andalusite, but there are differences between the XRD patterns. The three principal peaks in sample 1 at $2\theta = 15.96^\circ$, 25.26° and 36.37° match the three andalusite {110}, {120} and {310} reflections. Two of the peaks in sample 1 approximately coincide with mullite, of which the major mullite peaks occur at $2\theta = 16.38^\circ$, 25.97° and 26.11° (JCPDF file #79-1455). The SEM image of sample 1 (Figures 5–1) reveals needle-shapes particles typical of mullite, suggesting that the transformation of andalusite to mullite has begun in this sample, resulting in a change in morphology and in the XRD pattern.

Table 3
Influence percentage of factors on parameters.

Factors	Additive		Al Source		Milling time	
Indexes	%	rank	%	rank	%	rank
Crystallinity	44	2	8	3	48	1
% X-Sialon	19	3	26	2	55	1
% Mullite	50	1	13	3	37	2
Response	23	3	26	2	51	1

Samples 2 and 3 are similar to sample 1 in being additive-free but differ in their source of Al and milling time. Firing of these two samples produces X-sialon and mullite, indicating that the milling time and the source of the aluminium content are parameters that influence the firing reactions. The XRD results (Fig. 2) suggest that sample 3 is the best in terms of the X-sialon content.

Samples 4, 5 and 6 contain Y_2O_3 as an additive, with different milling times and sources of Al. The degree of crystallinity in these samples is lower than in additive-free samples and samples containing TiO_2 additive (Fig. 2). The presence of Y_2O_3 leads to an increase in the content of molten phases content, increasing the amorphous component. Comparison between the Al_2O_3–SiO_2–Y_2O_3 [17] and Al_2O_3–SiO_2–TiO_2 [18] ternary phase diagrams shows that in the Y_2O_3-containing samples (Table 2),

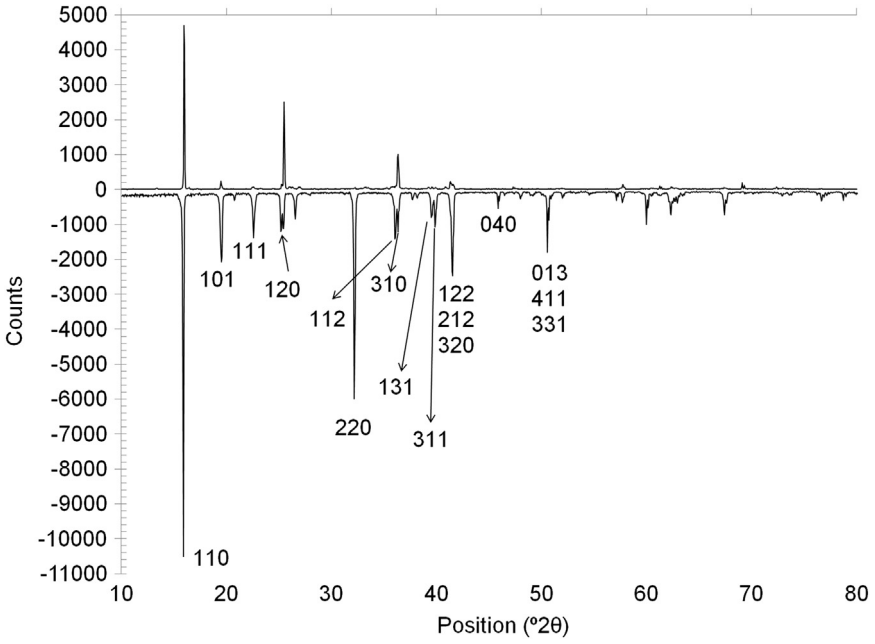

Fig. 4. The comparison between sample 1 (upper) and the andalusite used as raw material (lower).

the eutectic point in this system is about 1400 °C whereas this eutectic temperature in TiO_2-containing samples (Table 2) is around 1470 °C. This difference leads to the formation of a greater content of amorphous phase in the Y_2O_3-containing samples. Sample 6 is exceptional, being formed under alumino-thermic conditions and containing β-sialon formation. This is reflected by its unique SEM image containing ~50 nm dia. nano-sized needle-shaped particles.

The SEM micrographs of samples 2 and 4 (Fig. 5) show the presence of bean-shaped particles; in accordance with EDS results in Table 4, the Al/Si ratios of these particles suggest they could correspond to X-sialon ($Si_6Al_{10}O_{21}N_4$, Al/Si ≈1.67). The SEM images also indicate that the porosity of sample 2 is greater than that of sample 4, related to the increased molten phase content promoted by the Y_2O_3. The SEM image of sample 5 shows sintered particles. The milling process leads to an increase in the amount of surface energy of the particles, so that in the presence of Y_2O_3, a molten phase is formed on the particle surfaces during firing, and after cooling, triple junctions are created between the particles.

Samples 7, 8 and 9 all contain TiO_2 additive but were prepared with different milling times and source of the aluminium component. The presence of the TiO_2 stabilises the mullite and increases the amount formed. It was hoped that the promotion by this additive of mullite formation from andalusite would facilitate X-sialon formation by further reaction with Si_3N_4, but it was found that the TiO_2 stabilized the mullite and hindered the formation of X-sialon. The TiO_2 mineralizer is located at the interface between the grains with molten shells, where interaction between the TiO_2 particles and the aluminosilicate relicts reduces the viscosity of the melt, thereby favouring mass transport. Ti enters into the mullite structure forming a Ti^{4+}-mullite solid solution [12]. The SEM images of samples 7, 8 and 9 all show similar semi-spherical particles related to the presence of the TiO_2. The 20 nm particle size of the TiO_2 ensured the presence of a large number of these particles to act as nucleation agents for mullite and other phases. The SEM image of sample 8 shows it to contain a large amount of 50 nm needle-like particles of mullite ($3Al_2O_3.2SiO_2$, Al/Si = 3) composition, according to their EDS results in Table 4. The TEM image and SAED pattern of this sample (Fig. 6) suggest that the cluster-shaped regions at the ends of these needles consist of amorphous phases from which the mullite has grown. The milling process and presence of TiO_2 leads to conjugate particles by the formation of a liquid phase during firing. The presence of a ~50 nm particle in the SEM of this sample suggests that this is the typical particle size range.

A careful investigation of the SEM images (Fig. 5) indicates that the synthesized powders show different morphology. In the lower magnification SEM images of samples 1, 6 and 8 (un-milled), micron sized particles are seen (not shown) whereas the SEM images of Fig. 5 show the surface of these particles. These three images are similar in containing needle-shaped grains. In other images, the porosity between grains is not as great as in the unmilled samples. SEM images of samples containing Al as the aluminium source (samples 3, 6 and 9) show semispherical shaped particles in the milled samples (Fig. 5 and Fig. 9) whereas the unmilled sample (Figs. 5 and 6) contains needle-shaped particles. It could be concluded that the chemical activity of the metallic Al during milling led to the formation of spherical agglomerates. The milling process and the addition of Y_2O_3 to samples 4 and 5 produced powder samples with the lowest degree of crystallinity , as clearly shown in Fig. 2. These observations suggest that the most influential parameters controlling the morphology of the specimens is the milling process, although the other factors should not be disregarded.

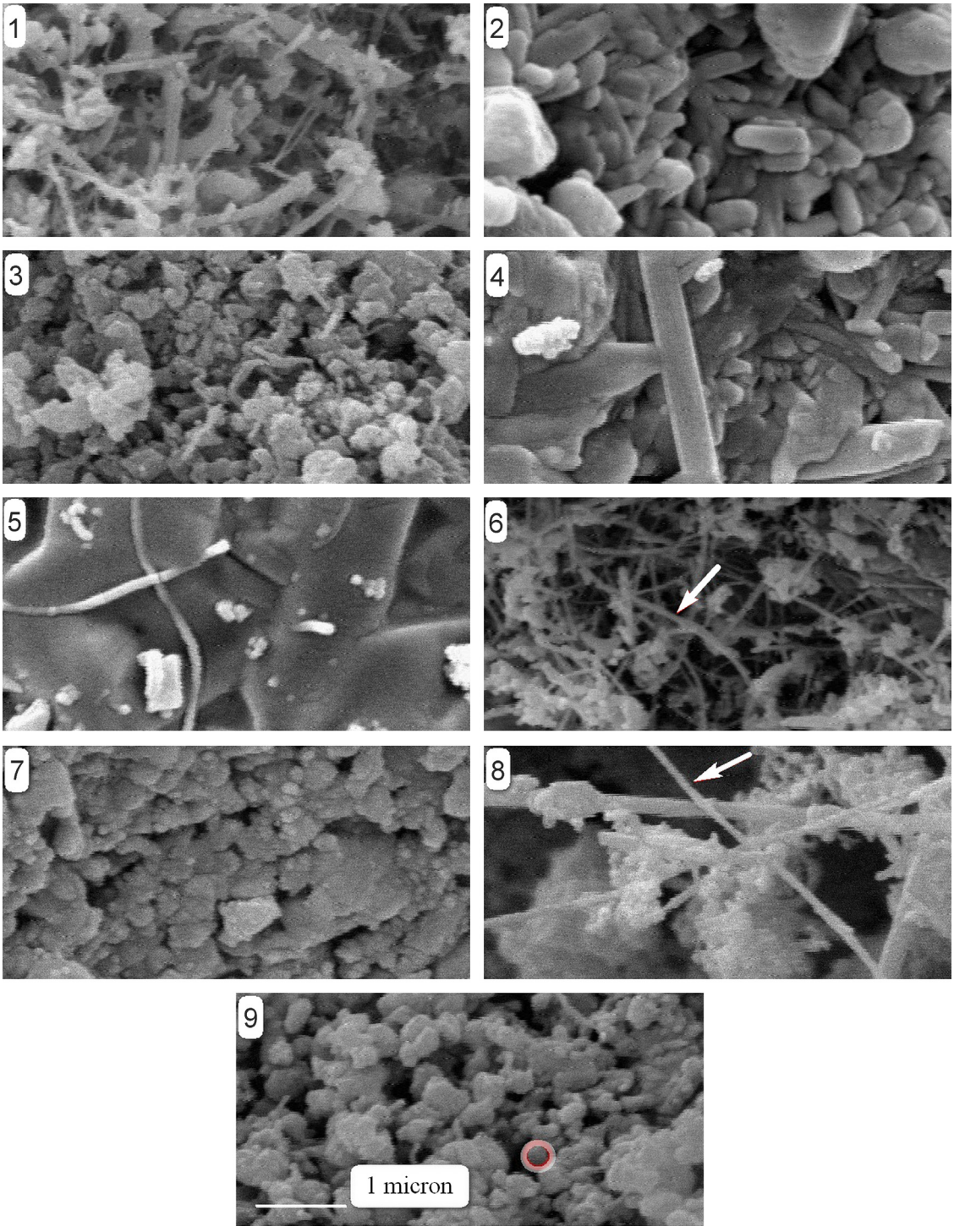

Fig. 5. SEM images of 9 samples.

Table 4
EDS results of selected points on samples providing the percentages of C, O, Al and Si atoms.

Sample	C	O	Al	Si	Al/Si
2	2.3	50.4	28.7	18.5	1.55
4	5.1	45.4	29.6	19.9	1.49
8	4.6	63.7	23.3	8.3	2.81

The additives, especially Y_2O_3, give rise to a liquid phase during firing. This suggests that the beneficial effects of Y are due to the formation of liquid phases at the reaction temperature, which facilitates the atomic movements, including bond breaking and reforming necessary to progress from mullite to X-sialon [6]. Although TiO_2 also produces liquid phases, Ti enters into the mullite structure forming a stable Ti^{4+}-mullite solid solution [12].

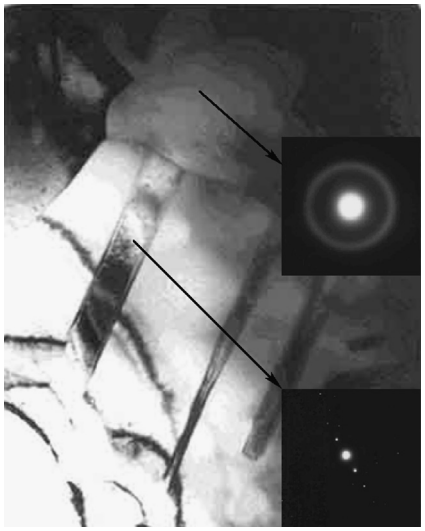

Fig. 6. TEM image of sample 8. The inset shows the SAED patterns of the cluster-shape region and particles of mullite.

X-sialon is the principal crystalline phase in samples 3 and 5, both of which were milled for 15 h, suggesting that this is an appropriate milling time for the formation of X-sialon. However, in sample 7, also milled for 15 h, very little X-sialon was formed, whereas mullite was the main crystalline phase (Fig. 2). In this sample, TiO_2 stabilizes the mullite and hinders X-sialon formation.

A statistical analysis of these results and discussion of the effect of the processing factors on the degree of crystallinity, percentage of X-sialon, percentage of mullite and response was carried out by the Taguchi method, as follows:

3.2. Degree of crystallinity

Fig. 3 and Table 3 show that the factor exerting the greatest effect on the degree of crystallinity is the milling time. Increasing the milling time from 0 to 15 h significantly decreases the degree of crystallinity, but further milling for 30 h produces little further change. The XRD traces of samples after grinding and prior to firing (not shown) indicate that no significant phase changes occurred during high-energy milling of the samples, but disintegration and plastic deformation with the formation of amorphous material gave rise to some line broadening and reduction in the height of the diffraction peaks as well as some decrease in the degree of crystallinity. The milling efficiency was high at the beginning of the process but gradually decreased, as previously explained by Emami et al. [19] who showed that the specific surface area of the particles increases during the grinding process. This increase in specific surface area is substantial at short grinding times but the rate gradually decreases, with a negligible change in the BET surface area after longer grinding times.

The second factor affecting the degree of crystallinity is the type of additive. The additive-free samples were more crystalline higher than those containing additives, with Y_2O_3 suppressing the crystallinity to a greater extent than TiO_2. This is related to the temperature of ternary eutectic temperatures as explained above [17,18]. Of the three sources of aluminium used here, elemental Al or Al_2O_3 produce samples of similar crystallinity, whereas $Al(OH)_3$ gives more crystalline samples. MacKenzie et al. have shown that grinding $Al(OH)_3$ with a silicate promotes the formation of Al–O–Si bonds [9], suggesting that the more crystalline product formed from $Al(OH)_3$ is related to the mechanochemical formation of Al–O–Si bonds from mullite or X-sialon crystallization.

3.3. Amount of X-sialon product

The factor exerting the greatest effect on the amount of X-sialon formed is the milling time. None of the unmilled samples (samples 1, 6 and 8) formed X-sialon even at the maximum firing temperature of 1450 °C, but this phase was formed after milling for 15 h which had the effect of activating the mixtures, thus providing appropriate conditions to form X-sialon at 1450 °C whereas Sheppard et al. reported that the minimum temperature required for X-sialon formation as the main phase is >1500 °C [5] . Doubling this milling time to 30 h produced no further increase in the amount of X-sialon formed, possibly related to the effect of the milling on the morphology of the particles (see below).

The amount of X-sialon formed is also influenced by the nature of the Al source used. The most X-sialon is formed from mixtures containing Al or Al_2O_3, whereas $Al(OH)_3$ exerted the least influence on X-sialon formation. As noted above, $Al(OH)_3$ increases the crystallinity, thus leading to a decrease in the amount of molten phase formed during firing and decreasing the diffusion distance in the system. Since X-sialon formation is diffusion-controlled [20], this effect decreases the amount of X-sialon formed.

The additives used exert only a slight effect on the formation of X-sialon. TiO_2 influences mullite formation by stabilizing this phase, and consequently the amount of X-sialon formed in the presence of TiO_2 is slightly decreased.

3.4. Amount of mullite formed.

Fig. 3 and Table 3 show that the factor exerting the greatest effect on the amount of mullite formed is the additive used. In the TiO_2-containing samples 7, 8 and 9, mullite is the main phase. The influence of TiO_2 on the formation of mullite has previously been reported by Montoya et al. [12] that was explained before. Very little mullite was formed in the additive-free samples and those containing Y_2O_3.

The second most important factor influencing mullite formation and stabilization is the milling time; more highly milled samples form more mullite (Fig. 3), contrary to X-sialon formation. X-sialon formation is a diffusion-controlled reaction [20] involving a gas diffusion step [5] whereas mullite formation is controlled by nucleation and growth [21] which may be related to the shape of the aggregated particles during milling and firing. The difference in these reaction mechanisms may explain the different behavior of mullite and X-sialon formation with milling time. Fig. 7 shows the SEM images of sample 2 milled for various times prior to firing. The unmilled

powder contains particles of large size and original shape (Fig. 7-A). Milling for 15 h leads to the formation of semi-spherical shaped particles (Fig. 7-B) whereas after milling for 30 h milling the particles are flake-shaped and agglomerated (Fig. 7-C). These flake-shaped agglomerates will decrease the diffusion of gas within the sample and suppress X-sialon formation, whereas the smaller particle sizes provide more sites for mullite crystallization. Thus, the amount of mullite formed in the samples milled for 30 h should be inversely dependent on the milling time.

The influence of the Al source on mullite formation is not as significant as the other factors, but Al_2O_3 is more stable to milling than the other forms of Al sources, and survives the milling process to react with amorphous SiO_2 in the system.

3.5. Response

The aim of this research was to obtain a highly crystalline composite containing a high concentration of X-sialon with a low concentration of other phases . To achieve this goal by optimizing the composition of the starting mixtures and other processing parameters, a parameter termed "Response" was defined as "the degree of crystallinity" multiplied by the "percentage of X-sialon" divided by the "percentage of mullite" (Eq. (1)). The processing factor that exerts the greatest effect on Response is seen from Fig. 3 to be the milling time. Thus, the present results indicate that the optimum compositions and processing parameters to produce composites with the desired properties are: milling time of 15 h, Al source of Al_2O_3, with Y_2O_3 (but not TiO_2) as an additive. Sample 5 of the present work conforms to these conditions.

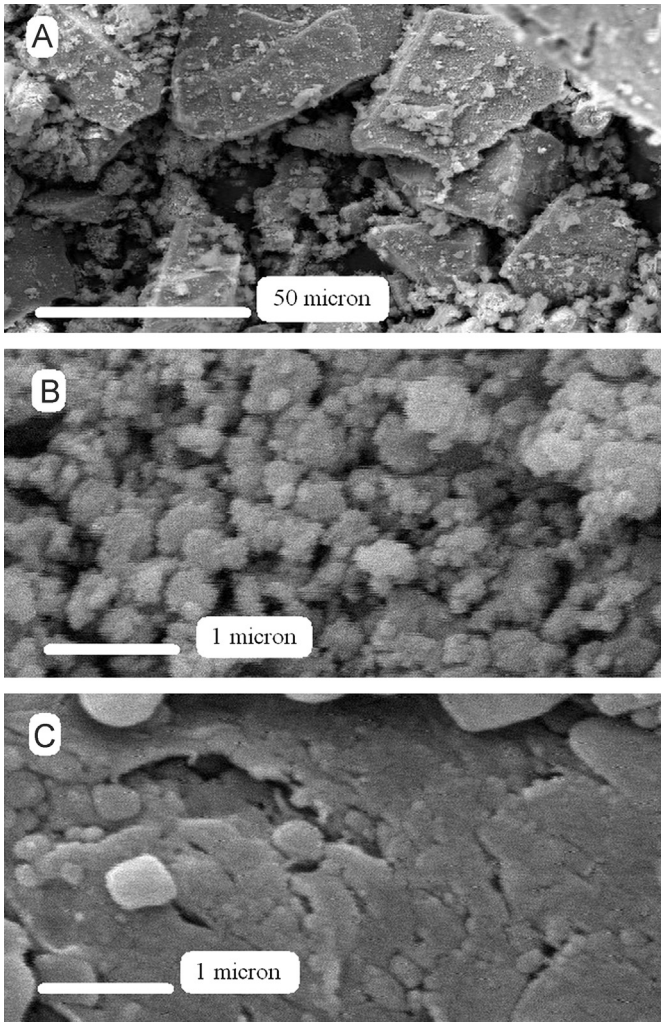

Fig. 7. SEM images of the green powder of sample 2. A: without milling. B: 15 h milling. C: 30 h milling.

4. Conclusion

Composites of mullite with X-sialon can be formed by nitridation of a highly milled mixture of andalusite with elemental Si and an aluminium source.

The milling time is the factor exerting the greatest influence on the formation and crystallinity of the X-sialon.

The nanocomposite powder obtained in this work after 15 h milling contains more X-sialon than in samples milled for 30 h.

The addition of TiO_2 to the mixture promotes the formation and stabilization of mullite whereas the addition of Y_2O_3 facilitates X-sialon formation.

Three different aluminium sources were used in this work, namely elemental Al, Al_2O_3 and $Al(OH)_3$. Of these, the latter increased the degree of crystallinity by facilitating the formation of Al–O–Si bonds during grinding.

The optimum processing conditions to achieve the goal of this research, namely a highly crystalline composite containing a high concentration of X-sialon with a low concentration of other phases, were found to be: a milling time of 15 h, Al source of Al_2O_3, with Y_2O_3 (but not TiO_2) as an additive.

References

[1] Y. Sakka, I.A. Aksay, Processing of nanocomposite silicon nitride–mullite–alumina by reaction sintering, NanoStructured Mater 4 (1994) 169–182.
[2] H. Wang, T. Sekino, K. Niihara, Z. Fu, Preparation of mullite-based iron magnetic nanocomposite powders by reduction of solid solution, Journal of Materials Science 44 (2009) 2489–2496.
[3] K.G.K. Warrier, G.M.A. Kumar, S. Ananthakumar, Densification and mechanical properties of mullite–SiC nanocomposites synthesized through Sol–Gel coated precursors, Bulletin of Material Science 24 (2001) 191–195.
[4] M. Albano, A.N. Scian, Mullite/SiAlON/alumina composites by infiltration processing, Journal of American Ceramics Society 80 (1997) 117–124.
[5] C.M. Sheppard, K.J.D. MacKenzie, G.C. Barris, R.H. Meinhold, A new silicothermal route to the formation of X-phase sialon: the reaction sequence in the presence and absence of Y_2O_3, Journal of the European Ceramic Society 17 (1997) 667–673.
[6] C.M. Sheppard, K.J.D. MacKenzie, Silicothermal synthesis and densification of X-sialon in the presence of metal oxide additives, Journal of the European Ceramic Society 19 (1999) 535–541.
[7] K.J.D. MacKenzie, C.M. Sheppard, C. McCammon, Effect of MgO, Y_2O_3, and Fe_2O_3 on silicothermal synthesis and sintering of X-sialon. An XRD, multinuclear MAS NMR and ^{57}Fe Mossbauer study, Journal of the European Ceramic Society 20 (2000) 1975–1985.
[8] A. Jamshidi, A.A. Nourbakhsh, M. Jafari, S. Naghibi, Combination of mechanical activation and silicothermal reduction and nitridation process

to form X-sialon by using andalusite precursor, Molecular Crystals and Liquid Crystals 555 (2012) 112–120.
[9] K.J.D. MacKenzie, J. Temuujin, M. Smith, K. Okada, Y. Kameshima, Mechanochemical processing of sialon compositions, Journal of the European Ceramic Society 23 (2003) 1069–1082.
[10] H. Pooladvand, B. Mirhadi, S. Baghshahi, A.R. Souri, K. Arzani, Effects of alumina and zirconia addition on transformation of andalusite to mullite, Advances in Applied Ceramics 108 (2009) 389–395.
[11] M. Bellotto, A. Gualtieri, G. Artioli, S.M. Clark, Kinetic study of the kaolinite–mullite reaction sequence. Part I: kaolinite dehydroxylation, Physics and Chemistry of Minerals 22 (1995) 207–217.
[12] N. Montoya, F.J. Serrano, M.M. Reventos, J.M. Amigo, J. Alarcon, Effect of TiO_2 on the mullite formation and mechanical properties of alumina porcelain, Journal of the European Ceramic Society 30 (2010) 839–846.
[13] R. Hagen, C. Lamy, B. Myhre, H. Peng, Mullite formation, high-temperature properties of andalusite–alumina based LCC and ULCC, in: Proceedings of the unified international technical conference on refractories; UNITECR, Salvador de Bahia, Brazil, October 13–16, 2009.
[14] K.H. Jack, Review, Sialon and related nitrogen ceramic, Journal of Materials Science 11 (1978) 1135–1158.
[15] B.D. Cullity, Elements of X-ray diffraction, 2nd edition, Addison-Wesley Publishing Company, Inc., Massachusetts, USA, 1956.
[16] F.H. Chung, Quantitative interpretation of X-ray diffraction patterns, I. matrix-flushing method of quantitative multicomponent analysis, Journal of Applied Crystallography 7 (1974) 513–519.
[17] A.M. Alper, Phase diagrams in advanced ceramics, 193, Elsevier, 2002.
[18] S.J. Li, F. Queyroux, Ph. Boch, Particulate composite in the Al_2O_3–SiO_2–TiO_2 system by infiltration processing, Journal of the European Ceramic Society 13 (1994) 3–9.
[19] A.H. Emami, M.Sh. Bafghi, J. Vahdati Khaki, A. Zakeri, The effect of grinding time on the specific surface area during intensive grinding of mineral powders, Iranian Journal of Materials Science and Engineering 6 (2009) 30–36.
[20] H. Kim, C.H. Kim, The effects of thermal diffusion of nitrogen gas on silicon nitridation rate, Journal of Materials Science Letters 3 (1984) 203–204.
[21] H. Schneider, K. Okada, J. Pask, Mullite and mullite ceramics, Wiley, Chichester, USA, 1994.